Int. J. Heat Mass Transfer. Vol. 31, No. 5, pp. 1049–1061, 1988
Printed in Great Britain

0017–9310/88 $3.00 + 0.00

Aiding and opposing mixed convection in a vertical porous layer with a finite wall heat source

F.-C. LAI
Department of Mechanical Engineering, University of Delaware, Newark, DE 19716, U.S.A.

V. PRASAD†
Department of Mechanical Engineering, Columbia University, New York, NY 10027, U.S.A.

and

F. A. KULACKI
Department of Mechanical Engineering, Colorado State University, Fort Collins, CO 80523, U.S.A.

(*Received* 10 *April* 1987 *and in final form* 7 *October* 1987)

Abstract—Two-dimensional, steady mixed convection in a vertical porous layer has been numerically studied for the case when a finite isothermal heat source is located on one vertical wall which is otherwise adiabatic and the other vertical wall is isothermally cooled. In the case of aiding mixed convection flow, the main flow separates from the cold wall and a recirculatory secondary flow exists in a region away from the heat source. However, when the main flow opposes buoyancy, the separation takes place on the heated wall, and the secondary flow is produced on the heated segment. Although the heat transfer rate increases with the aiding velocity, the effect is small at lower Peclet numbers (*Pe*). For the aiding flow, the slope of the Nusselt number curve increases with Peclet number unless the flow has approached the forced convection regime. For opposing flow, the heat transfer rate first decreases with an increase in *Pe* beyond zero and reaches a minimum before it starts increasing again. Under certain circumstances, the Nusselt number for a lower Rayleigh number may exceed that for a higher *Ra*.

1. INTRODUCTION

INTEREST in understanding the convective transport processes in porous materials is rapidly increasing because of the development of geothermal energy technology, thermally-enhanced oil recovery, high performance insulation of building and cold storage, renewed interest in energy-efficient drying processes, transpiration cooling, powder metallurgy and many other areas. Some of its direct technological applications are the underground spread of pollutants, insulation of buildings and pipes, design of regenerative heat exchangers, thermal energy storage, drying processes in the food and paper industries, dynamics of avalanches in snow layers, chemical catalytic reactors, and storage of nuclear wastes in a geologic repository. This has led to a large volume of research on free and forced convection in porous media in the last 40 years. The motivation for the present study comes from the fact that both free and forced convection may exist simultaneously in many of the aforementioned applications. This is particularly relevant in situations where the Grashof number is large, e.g. in petroleum recovery processes where buoyancy-induced flow can become very important.

A survey of the literature on convective heat transfer in porous media reveals that few efforts have been made to study combined free and forced convection in saturated porous media. Wooding [1] conducted the first study on mixed convection in a porous layer which was later followed by Prats [2], Elder [3], and Combarnous and Bia [4]. Jannot *et al.* [5] and Burns *et al.* [6] considered the effect of forced flow on natural convection in a vertical slot. Cheng and co-workers [7–11] conducted a series of investigations to study mixed convection over vertical, inclined and horizontal impermeable plates. Recently, Ranganathan and Viskanta [12] have examined the boundary and inertia effects on mixed flow along a vertical surface. Studies relevant to a geothermal reservoir have been reported by Horne and O'Sullivan [13], Cheng and co-workers [14, 15], Schrock and Laird [16], and Troncoso and Kassoy [17]. Mostly, these studies are limited to either similarity and numerical solutions for external flows or onset of convection in bounded porous media.

Extensive numerical investigations to examine buoyancy effects on forced flow through a horizontal porous layer with a finite heat source on the bottom surface have recently been conducted by the present authors [18–20]. Oosthuizen [21] has considered the mixed flow over a heated, horizontal plate near an impermeable, adiabatic horizontal surface. The

† Author to whom correspondence should be addressed.

NOMENCLATURE

C	specific heat of fluid at constant pressure [J kg^{-1} K^{-1}]
d	particle size [m]
Da	Darcy number, K/L^2
g	acceleration due to gravity [m s^{-2}]
Gr	Grashof number for the porous medium, $g\beta KL\Delta T/\nu^2$
H	length of the heat source [m]
H_1	channel height on the lower side of the heat source (in the computational domain) [m]
H_2	channel height on the upper side of the heat source (in the computational domain) [m]
h	local heat transfer coefficient for the heated segment [W m^{-2} K^{-1}]
$\bar{h}$	average heat transfer coefficient for the heated segment [W m^{-2} K^{-1}]
K	permeability of saturated porous medium [m^2]
k	effective thermal conductivity of porous medium [W m^{-1} K^{-1}]
L	vertical channel width [m]
Nu	local Nusselt number, hL/k
$\overline{Nu}$	overall Nusselt number based on layer width, $\bar{h}_d L/k$
p	pressure [Pa]
Pe	Peclet number for porous medium, VL/α
Pr	Prandtl number for porous medium, ν/α
Ra	Rayleigh number for porous medium, $g\beta KL\Delta T/\nu\alpha$
Re	Reynolds number based on channel width, VL/ν
Re_d	particle Reynolds number, Vd/ν
T	temperature [K]
ΔT	temperature difference, $(T_h - T_c)$ [K]
u	fluid velocity in x-direction [m s^{-1}]
u'	dimensionless velocity in x-direction, $u/V = -(\partial\psi/\partial Y)$
v	fluid velocity in y-direction [m s^{-1}]
v'	dimensionless velocity in y-direction, $v/V = (\partial\psi/\partial X)$
V	externally-induced velocity [m s^{-1}]
x,y	Cartesian coordinates [m]
X	dimensionless distances on x-axis, x/L
Y	dimensionless distances on y-axis, y/L
Y_1	dimensionless distances on the lower side of the heat source, H_1/L
Y_2	dimensionless distances on the upper side of the heat source, H_2/L.

Greek symbols

α	thermal diffusivity of porous medium, $k/\rho C$ [m^2 s^{-1}]
β	isobaric coefficient of thermal expansion for fluid [K^{-1}]
ε	porosity
θ	dimensionless temperature, $(T-T_c)/(T_h-T_c)$
ν	kinematic viscosity of fluid [m^2 s^{-1}]
ρ	density of fluid [kg m^{-3}]
ψ	dimensionless stream function.

Subscripts

att	reattachment point
c	cooled wall
cr	critical value
FC	forced convection
h	heated segment
MC	mixed convection
max	maximum
min	minimum
NC	natural convection
r	reference point
sep	separation point
y	local value on the vertical wall.

interaction between a horizontal through-flow and a buoyant flow driven by a horizontal temperature gradient has been examined by Haajizadeh and Tien [22]. In contrast, limited efforts have been made to study the combined free and forced convection in vertical porous layers where the forced flow either aids or opposes the buoyancy-induced flow. Indeed, only Parang and Keyhani [23] have considered the fully-developed buoyancy-aided mixed convection in an annular porous layer with uniform heating on the inner and/or outer wall.

The purpose of the present work is to examine the interaction between an upward or downward through-flow in a vertical porous layer, and a buoyant flow induced by a finite heat source on one bounding wall. The problem is of significant importance to many geophysical and engineering-related applications. The recent motivation to study mixed convection from a localized heat source has also come from the efforts to accurately predict the thermal and hydraulic response of a nuclear waste repository to the fluid flow through the surrounding permeable medium.

2. FORMULATION

The model comprises a two-dimensional isotropic, homogeneous porous layer bounded by two impermeable vertical walls as shown in Fig. 1. A finite isothermal heat source of length, H, is located on one vertical wall which is adiabatic elsewhere. The other

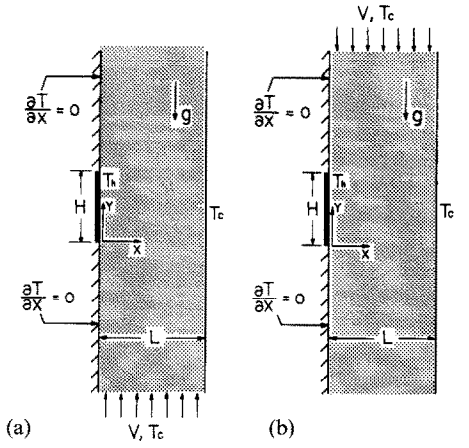

FIG. 1. Two-dimensional vertical porous layer with a finite isothermal heat source of length $H = L$, coordinate systems and boundary conditions: (a) aiding flow; (b) opposing flow.

vertical wall of the channel is maintained at a temperature, T_c, which is less than the temperature of the heat source, T_h. An externally-induced flow is maintained through this porous channel either upward or downward. It is assumed that far away from the heat source on the upstream side, the cold fluid is at a constant temperature, T_c, and flows with a uniform velocity, V.

Darcy's law together with the Boussinesq approximation and negligible thermal dispersion produces the following governing equations:

$$\frac{\partial u}{\partial x}+\frac{\partial v}{\partial y}=0 \tag{1}$$

$$u=-\frac{K}{\mu}\frac{\partial p}{\partial x} \tag{2}$$

$$v=-\frac{K}{\mu}\left(\frac{\partial p}{\partial y}+\rho g\right) \tag{3}$$

$$u\frac{\partial T}{\partial x}+v\frac{\partial T}{\partial y}=\alpha\left[\frac{\partial^2 T}{\partial x^2}+\frac{\partial^2 T}{\partial y^2}\right] \tag{4}$$

$$\rho=\rho_r[1-\beta(T-T_r)]. \tag{5}$$

The relevant boundary conditions (Fig. 1) are given by

$$u=0,\quad T=T_h,\quad x=0,\quad 0\leqslant y\leqslant H \tag{6a}$$

$$\partial T/\partial x=0,\quad x=0,\quad y<0,\ y>H \tag{6b}$$

$$u=0,\quad T=T_c,\quad x=L,\quad -\infty<y<\infty \tag{6c}$$

$$v=V,\quad T=T_c,\quad y\to-\infty,$$

$$v=V\quad \partial T/\partial y=0,\quad y\to\infty,$$

$$\left.\begin{array}{ll}0<x<L & \text{aiding}\\ 0<x<L & \text{flow}\end{array}\right\} \tag{6d, 6e}$$

$$v=V,\quad T=T_c,\quad y\to\infty,$$

$$v=V,\quad \partial T/\partial y=0,\quad y\to-\infty,$$

$$\left.\begin{array}{ll}0<x<L & \text{opposing}\\ 0<x<L & \text{flow.}\end{array}\right\} \tag{6f, 6g}$$

Here, it has been assumed that far away from the heat source on the downstream side the flow will become parallel, and the axial conduction will be almost negligible (equations (6e) and (6g)).

With length scales V (velocity), L (length), and T_h-T_c (temperature), equations (1)–(5) are transformed to obtain

$$\frac{\partial^2\psi}{\partial X^2}+\frac{\partial^2\psi}{\partial Y^2}=\frac{Ra}{Pe}\frac{\partial\theta}{\partial X} \tag{7}$$

$$\frac{\partial\psi}{\partial X}\frac{\partial\theta}{\partial Y}-\frac{\partial\psi}{\partial Y}\frac{\partial\theta}{\partial X}=\frac{1}{Pe}\left(\frac{\partial^2\theta}{\partial X^2}+\frac{\partial^2\theta}{\partial Y^2}\right). \tag{8}$$

Boundary conditions (6a)–(6g) reduce to

$$\psi=0,\quad \theta=1,\quad X=0,\quad 0\leqslant Y\leqslant 1 \tag{9a}$$

$$\partial\theta/\partial X=0,\quad X=0,\quad Y<0,\ Y>1 \tag{9b}$$

$$\psi=0,\quad \theta=0,\quad X=1 \tag{9c}$$

$$\psi=X,\quad \theta=0,\quad Y=-Y_1 \text{ aiding} \tag{9d}$$

$$\partial\theta/\partial Y=0,\quad Y=Y_2 \text{ flow} \tag{9e}$$

$$\psi=-X,\quad \theta=0,\quad Y=Y_2 \text{ opposing} \tag{9f}$$

$$\partial\theta/\partial Y=0,\quad Y=-Y_1 \text{ flow} \tag{9g}$$

where Y_1 and Y_2 are taken large enough such that the assumed boundary conditions (equations (6d)–(6g)) are realistic.

3. NUMERICAL METHOD

In the present numerical scheme, the stream function and temperature equations (7) and (8) are transformed into finite-difference equations by integration over finite area elements. This approach ensures that the conservation laws are obeyed over arbitrarily large or small portions of the domain. Integration of the equations in a way as outlined by Spalding and coworkers [24] introduces upwind differences for the convective terms in the energy equation, and is equivalent to second upwind differencing. The successive substitution formulae derived in this way satisfy the convergence criterion and is stable for many circumstances. For solving the system of algebraic equations thus obtained, a point iterative method is employed which makes use of the new values as soon as they are available. Successive-over-relaxation of temperature further enhances convergence. The solution technique is described well in the literature and has been successfully used by the present authors and others for convective heat transfer in porous media.

As discussed earlier, the choice of the length of unheated sections before and after the heat source (in the computational domain) are of considerable importance to satisfy the boundary conditions (equations (9d)–(9g)). Several trial runs were thus conducted for various combinations of Ra and Pe to select proper values of Y_1 and Y_2, and mesh size. One such trial run for an appropriate grid-field is shown

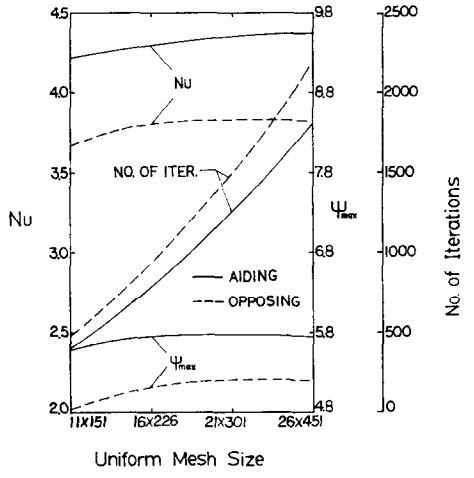

FIG. 2. Effect of mesh size on Nusselt number, maximum stream function and number of iterations for $Ra = 50$ and $Pe = 1$.

in Fig. 2 for $Ra = 50$ and $Pe = 1$. Clearly, a grid-field of 21×301 can be expected to yield reasonably accurate results for this Rayleigh number. Nevertheless, the length on the upstream and downstream sides of the heat source, i.e. Y_1 and Y_2, have been varied as functions of Peclet number and flow direction. For large Peclet numbers, a longer downstream side is considered to accurately predict the temperature and flow fields and satisfy the boundary conditions.

For the present computations, 21×201, 21×301 and 21×401 uniform meshes have been used for $Ra = 10$, 50 and 100, respectively. It should be noted that the consideration of non-uniform grids for these number of nodes did not produce any significant improvement in the results. A variation of 10^{-4} or less in the local values of both θ and ψ at all nodes in the computational domain was found to be adequate. This generally requires 1000–2500 iterations for the present range of parameters with the opposing flow requiring more iterations than aiding flow.

To further check the accuracy of the numerical results, an overall energy balance is used for the system. This compares the energy gained by the convective medium from the heat source with the heat removed on the cold wall plus the energy being carried away by the fluid at the downstream boundary of the channel in the computational domain. For a large number of calculations (over 50%), the energy balance is satisfied within 1%, whereas for the rest, it is well within 2%. Further details of the numerical scheme are omitted here for brevity and may be found in refs. [19, 25].

4. RESULTS AND DISCUSSION

Results have been obtained for $Ra = 10$, 50 and 100, and $0.01 \leqslant Pe \leqslant 100$, for both aiding and opposing flows† when the length of the heated segment equals the layer width, i.e. $H = L$. Computations have also been carried out to obtain heat transfer results for forced convection for $1 \leqslant Pe \leqslant 100$.

4.1. *Velocity and temperature fields: aiding flow*

In the absence of a through-flow in a vertical channel, it is expected that a recirculatory flow motion will be induced by the isolated heat source in the vertical channel since the opposite wall of the channel is isothermally cooled. This is also evident from the work of Prasad *et al.* [26] on free convection from a finite wall heat source in a vertical cavity. It is obvious that the higher the Rayleigh number, the stronger will be the recirculating flows and the larger will be the extent of the convective cell. However, the convective cell will extend much more on the upper side of the heat source than below it [26].

The buoyancy-induced flow pattern is significantly modified if an external pressure gradient causes the fluid to flow upward. When the forced flow is weak, buoyant effects still dominate the velocity field. However, the acceleration caused by the buoyant forces deflect the main flow toward the heat source causing a separation from the cold wall in the lower portion of the channel, i.e. on the upstream side (Fig. 3(a)).‡ The vertical velocity in a thin layer on the heated segment thus increases (Fig. 5), and the thermal convection on downstream side is enhanced. The aiding flow, however, reattaches to the cold wall far downstream (away from the heat source) after rejecting a large fraction of heat to the cold wall.

Figures 3(a)–(d) and 4(a)–(d) demonstrate the effect of Peclet number on the velocity and temperature fields for a fixed Rayleigh number, $Ra = 50$. An increase in the externally-induced velocity, V (or Peclet number, Pe), is observed to move the convective cell upward. This delays the separation of the main flow from the cold wall (Figs. 3(a)–(d)). When the Peclet number is high, the increase in the relative strength of forced and buoyancy-induced flows diminishes the adverse pressure gradient near the cold wall. Also, the enhanced thermal convection in the upward direction, as compared to that across the channel, weakens the negatively buoyant effects on the cold wall. As a result, the strength of the secondary flow decreases substantially, and the reattachment point moves upstream with an increase in Peclet number (Figs. 3(a)–(d)). Also, the eye of the cell is pushed toward the cold wall.

Finally, at a higher Peclet number ($Pe > 10$), the main flow does not separate from the cold wall and the effects of buoyant forces become negligible in com-

† The flow is referred to as 'aiding' when the external flow aids the buoyancy forces on the hot wall. The opposing flow thus represents the situation when the buoyant flow on the hot wall is opposed by the forced flow.

‡ The entire computational domain has not been shown in the streamline and isotherm plots presented in Figs. 3, 4, and 6–8.

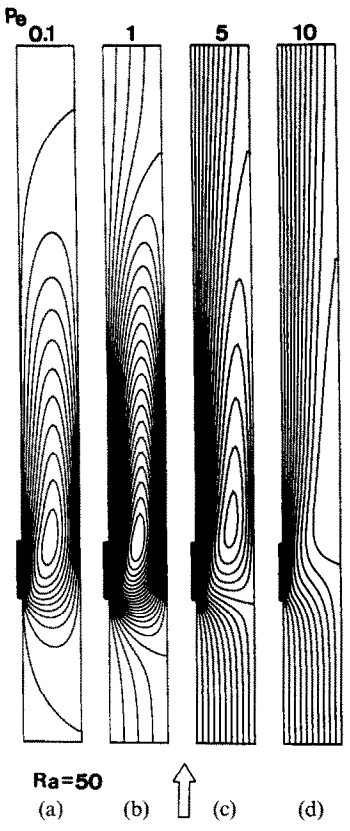

FIG. 3. Streamlines for $Ra = 50$, aiding flow: (a) $Pe = 0.1$ ($\Delta\psi = 5$); (b) $Pe = 1$ ($\Delta\psi = 0.25$); (c) $Pe = 5$ ($\Delta\psi = 0.1$); (d) $Pe = 10$ ($\Delta\psi = 0.1$). Streamlines for external flow cannot be seen in (a) since $\Delta\psi \geqslant 1$.

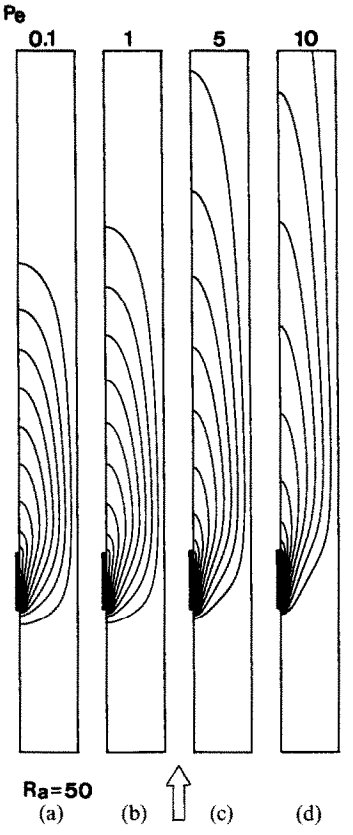

FIG. 4. Temperature field for $Ra = 50$, aiding flow ($\Delta\theta = 0.1$): (a) $Pe = 0.1$; (b) $Pe = 1$; (c) $Pe = 5$; (d) $Pe = 10$.

parison with the forced convection. This is characterized by thermal convection in a much larger domain and a fully developed flow on the downstream side. Figure 5 further demonstrates that the velocity on the heated wall is increased with Peclet number, whereas the effect is just the opposite on the cold wall. Also, the velocity profiles in the wall region are almost linear at all Peclet numbers.

To further demonstrate the effect of Rayleigh number on the cellular flow pattern and convective effects on the downstream side, the velocity and temperature fields for $Ra = 10$ and $Pe = 1$ are presented in Fig. 6(a). As expected, the domain of the recirculating flow increases with Rayleigh number (compare Figs. 6(a) and 3(b)), and the separation point moves upstream while the reattachment point moves downstream with Ra. The temperature fields in Figs. 6(a) and 4(b) further show that the convection on the downstream side is significantly enhanced with an increase in the buoyancy effects.

4.2. *Velocity and temperature fields: opposing flow*

Figures 7(a)–(c) and 8(a)–(c) demonstrate the effect of Peclet number on the streamline and isotherm patterns, respectively, for the case when the externally-induced flow is downward. When the main flow is weak, the buoyancy causes an upward flow in a region close to the heated segment. A recirculating flow is then produced in the hot wall region and the downward main flow is deflected towards the cold wall (Figs. 7(a)–(c)). This is contrary to what has been observed in the case of aiding flow.

When the Peclet number is small, the secondary flows for both aiding and opposing mixed convection, are close to each other in strength and extent (Figs. 3(a) and 7(a)). However, an increase in Pe for opposing mixed flow substantially reduces the strength and size of the convective cell. The upward vertical velocity decreases in a region close to the heated wall while the downward velocity on the cold wall increases with Pe (Fig. 9). In fact, the velocity distribution changes significantly by the reversal of the main flow (Figs. 6 and 9). An increase in Peclet number then moves the separation and reattachment points closer to the heat source, the effect being substantial on the separation point.

The temperature field is also modified significantly with the change in the direction of the main flow (Figs. 4 and 8). An increase in Peclet number now moves the thermal plume downward, closer to the heat source, rather than moving it upward as in the case of aiding flow. As a result, the region of intense thermal activity shrinks substantially with the increase in Peclet number. For example, the isotherms for $Ra = 50$, $Pe = 5$ (Fig. 8(b), $\theta > 0.1$) extend to only

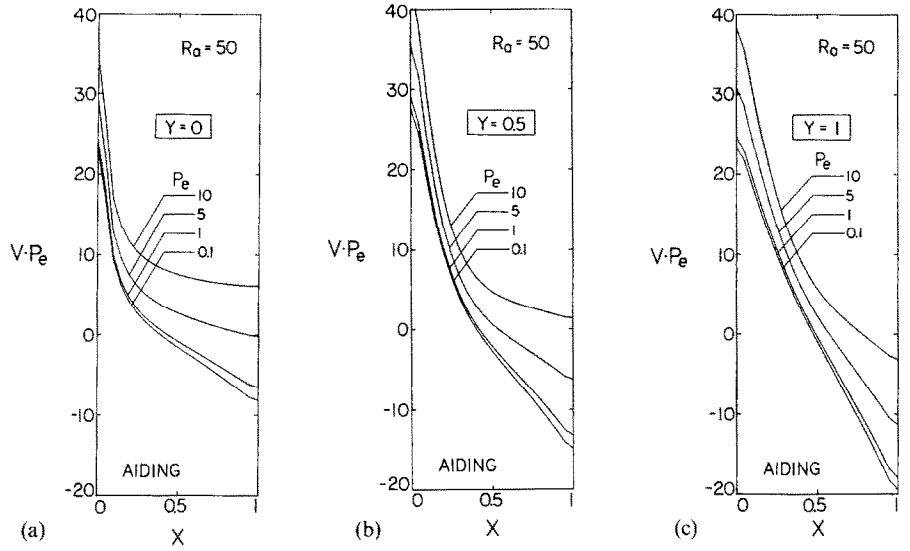

FIG. 5. Vertical velocity for various Peclet numbers, aiding flow: (a) $Y = 0$; (b) $Y = 0.5$; (c) $Y = 1$.

about one and a half times the heater length on both sides of the heat source. Consequently, the heat transfer rate is reduced from its free convection value for $Pe > 0$. However, above a certain Peclet number, the recirculating flow disappears, and the heat transfer coefficient increases with Pe. The critical Peclet number for the disappearance of secondary flow is a strong function of Rayleigh number.

The effect of Rayleigh number on the velocity and temperature fields for the opposing flow are demonstrated in Fig. 6(b) together with Figs. 7(b) and 8(b). Figure 6(b) shows that the streamline and isotherm patterns for $Ra = 10$ and $Pe = 1$ are almost symmetric about $Y = 0.5$. This symmetric property of the flow and temperature fields cannot be observed in the case of aiding flow (Fig. 6(a)), and is completely destroyed with an increase in the buoyancy effects even for opposing flow (Fig. 8(b)). Indeed, this symmetric nature of the temperature and velocity fields is characteristic of the balance between the external pressure gradient and the buoyant forces, and will be exhibited by only a particular Peclet number for a fixed Rayleigh number or vice versa.

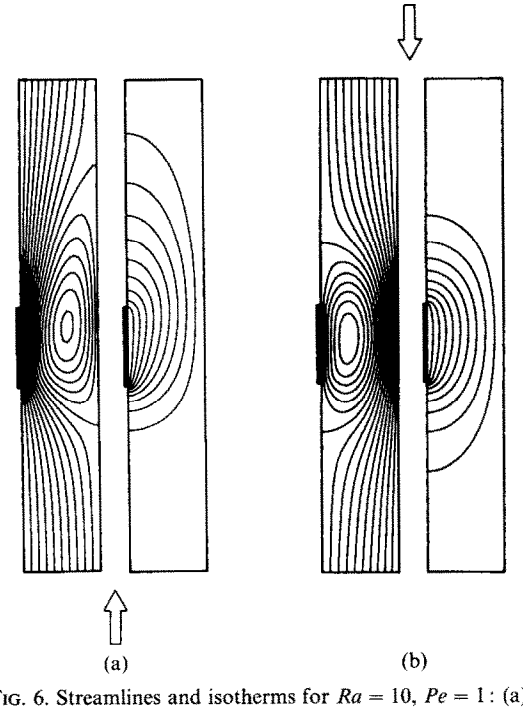

FIG. 6. Streamlines and isotherms for $Ra = 10$, $Pe = 1$: (a) aiding flow; (b) opposing flow ($\Delta\psi = 0.1$, $\Delta\theta = 0.1$)

4.3. *Separation and reattachment*

As shown earlier, if the buoyant forces are strong, the main flow may separate from one of the side walls of the channel and reattach it afterwards. Figure 10(a) shows that the separation point on the cold wall is always closer to $Y = 0$ (the leading edge) than the reattachment point to $Y = 1$ (the trailing edge). Although the reattachment point moves away from the top edge of the heat source, $Y = 1$, with an increase in Ra, the effect of Rayleigh number on the separation point is minimal. The curve for Y_{sep} vs ln (Pe) is almost a straight line when $Pe < 1$. A similar linear distribution is exhibited by the curve for reattachment points for low Peclet numbers, $Pe < 0.1$.

The plots for opposing flow (Fig. 10(b)) show almost identical linear distributions of the separation and reattachment points for low Peclet numbers. However, there exists a major difference between the two cases that the separation now occurs on the upper side of the heating element and the reattachment on the lower side. Figures 10(a) and (b) further demonstrate that the separation points for the aiding flow are within 2% of the reattachment points for the opposing flow, for fixed values of Ra and Pe (< 1). Similarly, the separation points for the opposing flow are up to 5% lower than the reattachment points for

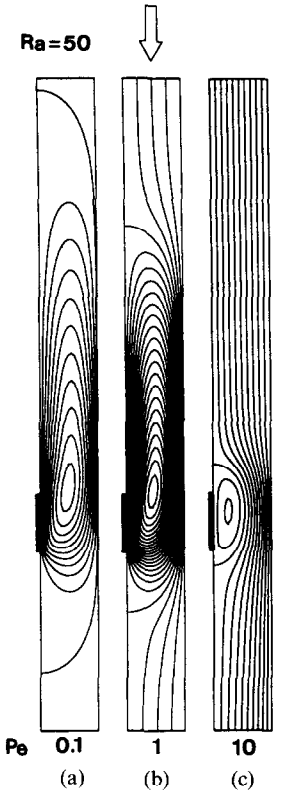

FIG. 7. Streamlines for $Ra = 50$, opposing flow: (a) $Pe = 0.1$ ($\Delta\psi = 5$); (b) $Pe = 1$ ($\Delta\psi = 0.25$); (c) $Pe = 10$ ($\Delta\psi = 0.1$). Streamlines for external flow cannot be seen in (a) since $\Delta\psi \geqslant 1$.

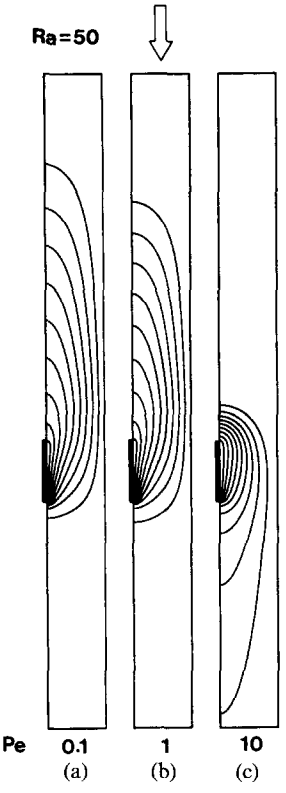

FIG. 8. Temperature field for $Ra = 50$, opposing flow ($\Delta\theta = 0.1$): (a) $Pe = 0.1$; (b) $Pe = 1$, (c) $Pe = 10$.

the aiding flow if $Pe < 0.1$. As mentioned earlier, this is a characteristic of the strong buoyant flows such that the natural recirculation remains almost unaffected by a variation in the direction of the main flow (Figs. 3(a) and 7(a)).

The reattachment curve for $Ra = 100$ in Fig. 10(a) further shows that the slope of this curve is reversed at $Pe \simeq 0.6$, i.e. the reattachment point moves upward with Peclet number for $Pe > 0.6$. However, at about $Pe \simeq 7$, the slope of this curve again becomes negative, and the reattachment point starts moving downward very sharply. Finally, the main flow does not separate from the vertical wall at $Pe \simeq 25$. Similar behavior is demonstrated by the curve for $Ra = 50$, but not by the curve for $Ra = 10$. Clearly, this depends on the relative strength of forced and buoyancy-induced flows, and can be observed only if both Ra and Pe are moderately large. As shown earlier, at a high Rayleigh number the buoyancy forces produce a strong convective cell whereas the external flow tries to destroy it. A balance between the two then results in an elongated, triangular cell near the cold wall with the reattachment point moved upward (Fig. 3(d)), and the strength of this cell reduced significantly. Consequently, the cell is diminished by even a small increase in Pe (Fig. 10(a)).

The similarity between the separation curve for the opposing flow and the reattachment curve for the aiding flow thus disappears at higher Peclet numbers. In fact, the two curves exhibit entirely opposite behavior when the external flow is strong. For the opposing flow, the separation point moves closer to the heating element at a faster rate when the Peclet number is increased beyond 0.1 (Fig. 10(b)). Nevertheless, the buoyancy-induced convective cell in the present case can exist at a higher Peclet number than in the aiding flow.

4.4. *Local heat transfer rates*

To demonstrate the variation in local heat transfer rate on the vertical walls, a local Nusselt number on the wall

$$Nu = hL/k = -\partial\theta/\partial X \tag{10}$$

has been calculated, and is plotted in Figs. 11 and 12 for both aiding and opposing flows. Figure 11 presents this Nusselt number for the heated segment whereas Fig. 12 shows the variation in Nu for the cold wall.

The Nusselt number curves for both aiding and opposing flows indicate that the heat transfer rate is maximum at the bottom edge of the heat source, $Y = 0$ (Figs. 11(a)–(d)), for all values of Ra and Pe. However, the Nusselt number decreases sharply with Y and reaches a minimum at the top edge, $Y = 1$. Generally, the variation in Nu over a large portion of the heated segment, is small.

For the aiding flow, the Nusselt number at any location Y, generally, increases with Rayleigh and/or

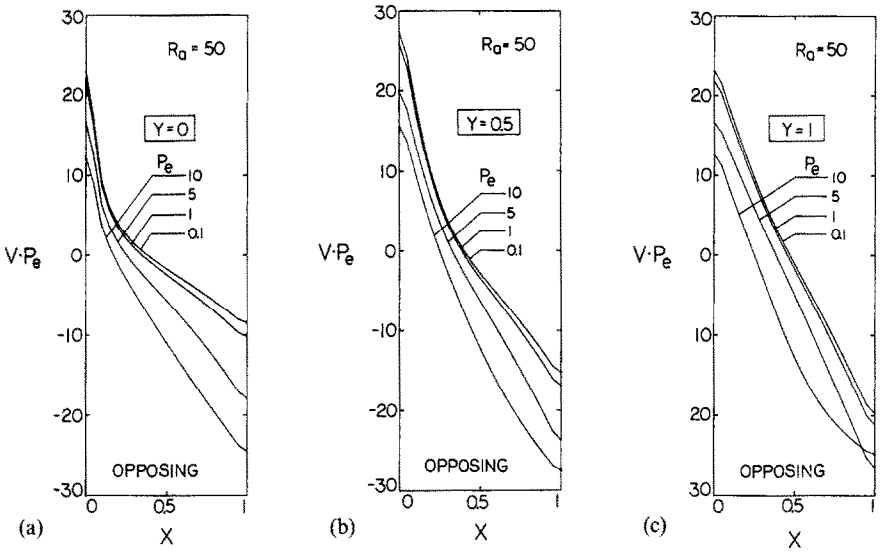

FIG. 9. Vertical velocity for various Peclet numbers, opposing flow: (a) $Y = 0$; (b) $Y = 0.5$; (c) $Y = 1$

Peclet number (Figs. 11(a) and (b)). However, if the Peclet number is not very high, an increase in the buoyant effects enhances heat transfer much more than a similar increase in the external velocity. For example, the variation in Nu for a ten-fold increase in Rayleigh number is much larger than that produced by an equal increase in the Peclet number. Similar effects of Rayleigh number are also observed in the case of opposing flow (Fig. 11(d)).

The effect of Peclet number on heat transfer rate is quite complex in the case of opposing flow. For a fixed Ra, the local Nusselt number initially decreases at all locations with an increase in Peclet number beyond zero. The effect is minimal near the upper end of the heat source, and is maximum at $Y = 0$. However, there exists a critical Peclet number as a function of Ra for which Nu at $Y = 1$ has the lowest value. Any increase in Pe beyond this critical Peclet number causes the Nusselt number at $Y = 1$ to increase with Pe. This reversal in local Nusselt number distribution with Pe is then observed at other locations in the top portion of the heated segment. The higher the Peclet number beyond Pe_{cr}, the larger is the area of the heated segment where Nu increases with Pe.

Figures 12(a)–(d) demonstrate that the higher the Peclet and/or Rayleigh number, the larger is the portion of the cold wall where heat is removed. The peak value of Nu for a fixed Ra, decreases with an increase in Pe because of the enhanced thermal convection on the downstream side (Fig. 12(a)). The effect of Rayleigh number is, however, not straightforward. There exists a critical Ra as a function of Pe for which Nu_{peak} is largest (Fig. 12(b)). A similar Rayleigh number effect is also observed in the case of opposing flow (Fig. 12(d)). Figure 12(c) further shows that Nu_{peak} decreases substantially with an increase in the external flow parameter, Pe.

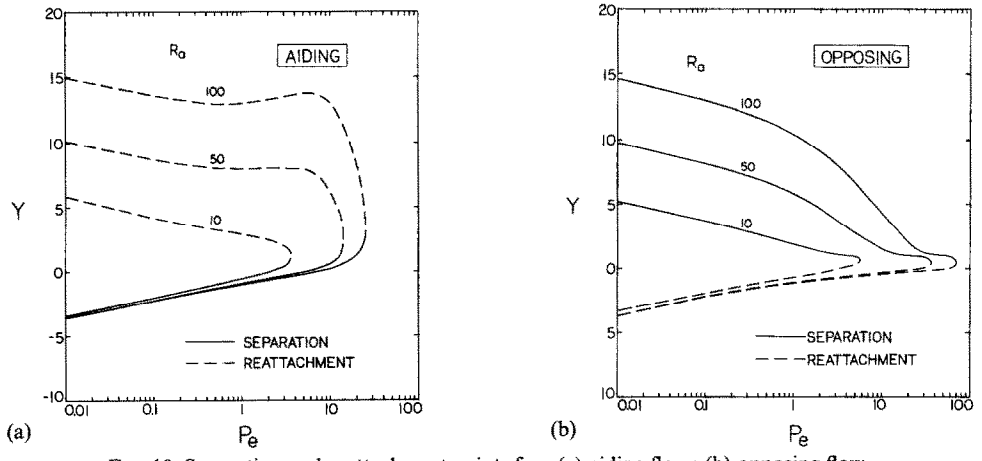

FIG. 10. Separation and reattachment points for: (a) aiding flow; (b) opposing flow.

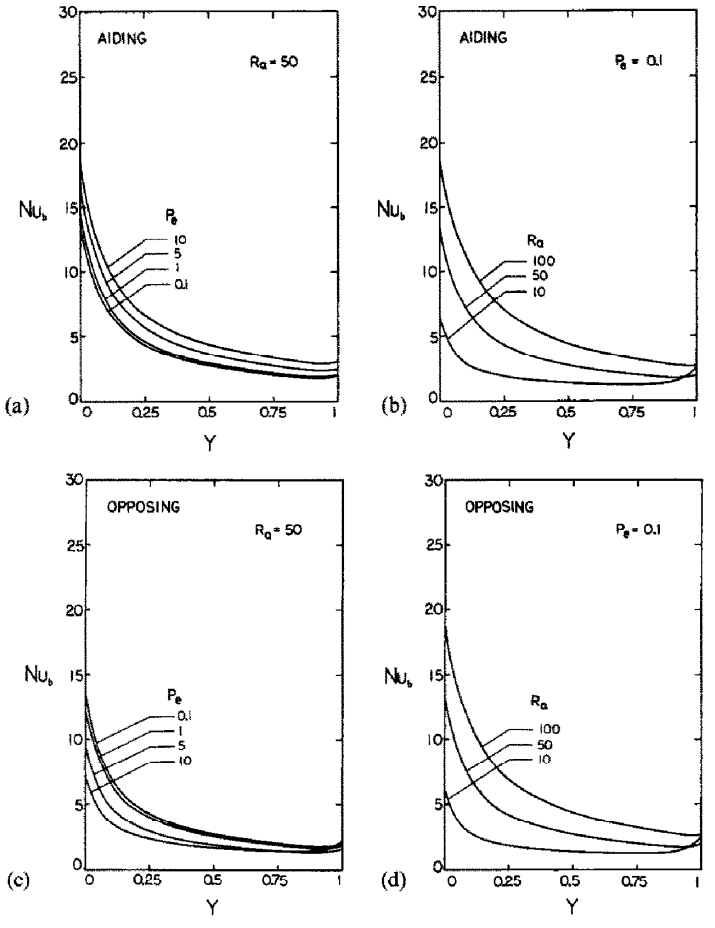

FIG. 11. Local Nusselt number on the heated segment. Aiding flow: (a) $Ra = 50$; (b) $Pe = 0.1$. Opposing flow: (c) $Ra = 50$; (d) $Pe = 0.1$.

4.5. *Overall heat transfer*

An average Nusselt number

$$\overline{Nu} = \bar{h}L/k = -\int_0^1 \left.\frac{\partial\theta}{\partial X}\right|_{X=0} \mathrm{d}Y \qquad (11)$$

has been calculated for both aiding and opposing flows, and is reported in Fig. 13 and Table 1. As long as the main flow aids buoyancy, $\overline{Nu}$ increases with Ra and/or Pe. For a fixed Ra, the Nusselt number has an asymptotic value in the free convection regime where the effects of forced flow are negligible.

For aiding flows, an increase in Peclet number beyond a certain value, however, results in an enhancement in heat transfer rate, and the slope of the Nusselt number curve starts increasing with Pe. With further increase in Peclet number, the value of the slope finally reaches a value close to 0.5, the slope reported for forced convection. The smaller the Rayleigh number, the earlier (in terms of Pe) the Nusselt number curve deviates from the free convection asymptote and the sooner it joins the forced convection curve. Figure 13 also shows the effect of Rayleigh number on the overall heat transfer rate, which is largest in the free convection regime, and diminishes with an increase in Peclet number.

The Nusselt number curve in Fig. 13 further indicates that the deviation from the free convection asymptote is a weak function of the direction of main flow, i.e. Nu deviates from the asymptotic value at almost the same Peclet number for both aiding and opposing flows. However, the heat transfer rate for the opposing flow may decrease with an increase in Peclet number (Fig. 13). The negative slope of the Nusselt number curve which is initially small, also increases with the external flow rate or Pe. The overall heat transfer rate, finally, reaches a minimum before it starts increasing with Pe. The higher the Rayleigh number, the larger is the Peclet number required for this inflection point.

Another interesting feature of Fig. 13 is that in the case of opposing flow, the Nusselt number for a lower Ra may exceed that for higher Rayleigh numbers in the mixed convection regime. For example, Nu for $Ra = 10$ is greater than that for $Ra = 50$ and 100 if $Pe > 20$. Figure 13 further indicates that this trend will continue unless the Peclet number is very high such that the buoyancy effects become negligible. Similar behavior has been demonstrated by the boundary layer solutions for a vertical plate [7].

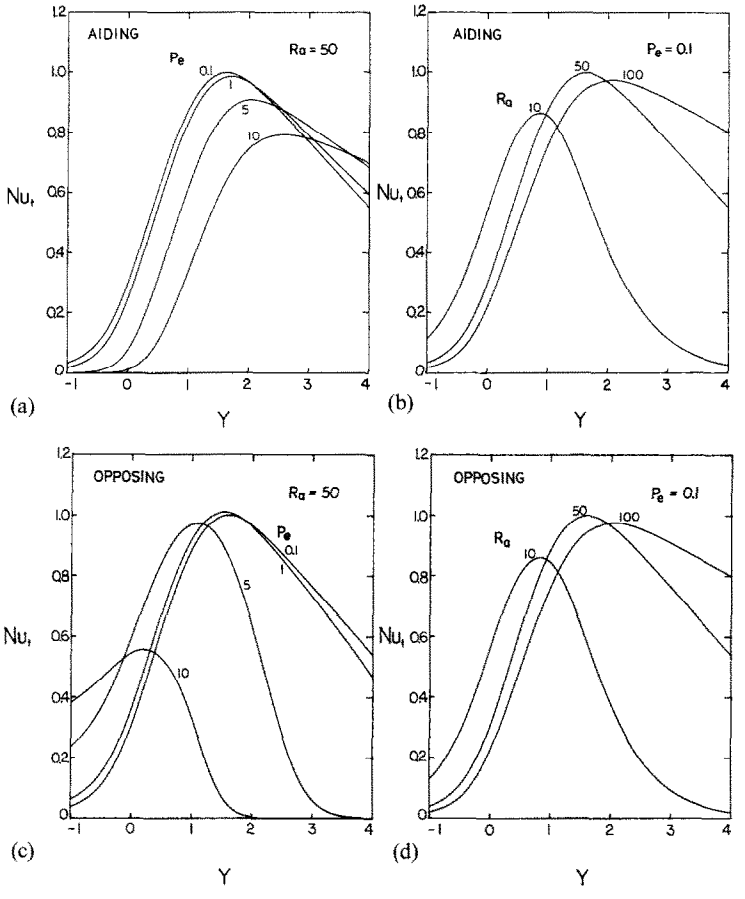

FIG. 12. Local Nusselt number on the cold wall. Aiding flow: (a) $Ra = 50$; (b) $Pe = 0.1$. Opposing flow: (c) $Ra = 50$; (d) $Pe = 0.1$.

Table 1 also presents the Nusselt numbers for forced convection which have been obtained by solving the energy equation (8) with $u = 0$ and $v = V$. These values of $\overline{Nu}$ support our earlier observation that the difference between $\overline{Nu}_{MC}$ and $\overline{Nu}_{FC}$ decreases with an increase in Peclet number and/or a decrease in Rayleigh number. To the authors' knowledge, there is nothing reported in the literature to which present heat transfer results can be directly compared. It is, however, of interest to compare these results with those reported for natural convection in a vertical cavity with a finite heat source on one wall [26], and for mixed flow on a fully-heated vertical plate [7]. Nusselt numbers reported by Prasad *et al.* [26] for the free convective heat transfer in a cavity of aspect ratio up to 5 are significantly higher (by about 25% at $Ra = 100$) than the present asymptotic values for free convection. However, the present results support the conclusion of Prasad *et al.* that the Nusselt number for free convection in a vertical cavity decreases from a peak to an asymptotic value as the aspect ratio approaches infinity. Evidently, the asymptotic Nusselt number for the geometry considered by them is the one obtained here for the free convection regime.

A comparison between the present results and the boundary layer solutions for an isothermally heated vertical plate embedded in a saturated porous medium at T_c [7], shows that the heat transfer from a flat plate is higher than that for a vertical channel if the forced flow is upward. The behavior is just the reverse in the case of opposing flow. The variation is largest in the free convection regime, and decreases with an increase in Peclet number (Table 1). The two Nusselt numbers are very close to each other in the forced convection regime. It may thus be concluded that in the boundary-layer forced convection regime, the flat plate solution of Cheng [7] can make reasonable predictions.

5. CONCLUSION

Numerical results have been reported for two-dimensional, steady mixed convection in a vertical porous layer for the case when a finite isothermal heat source is located on one vertical wall of the channel which is otherwise adiabatic. The other vertical wall has been assumed to be isothermally cooled, and the length of the heated segment equals the channel width.

In the mixed convection regime, the main flow separates from the vertical wall, reattaches afterwards, and produces a recirculating, secondary flow in the channel. When the flow is upward, separation and

Table 1. Present average Nusselt numbers compared with the boundary layer solutions for the vertical plate [7]

Flow	*Ra*	*NC*	*Pe* = 0.01	*Pe* = 0.1	*Pe* = 1		*Pe* = 5		*Pe* = 10		*Pe* = 50		*Pe* = 100	
		VP	VC	VC	VC	VP	VC	VP	VC	VP	VC	VP	VC	VP
Aiding flow	10	2.80	2.08	2.09	2.27	3.03	3.23	3.67	4.22	4.56	8.43	9.15	11.63	11.80
	50	6.28	4.07	4.09	4.33	6.30	5.31	6.78	6.23	7.08	9.84	10.19	12.63	12.95
	100	8.88	6.34	6.36	6.57	8.88	7.43	9.24	8.26	9.59	11.41	11.60	13.84	14.41
Opposing flow	10	2.81	2.08	2.06	1.96		2.32		3.22	2.10	7.73	7.45	11.08	10.90
	50	6.28	4.06	4.04	3.80		2.83		2.41		6.20	4.70	9.86	10.54
	100	8.88	6.34	6.32	6.10		5.16		4.17		4.63		8.28	6.64
Forced convection					1.96		2.72	2.52	3.70	3.57	8.10	7.98	11.38	11.28

Note: VC = vertical channel (present study); VP = vertical plate.

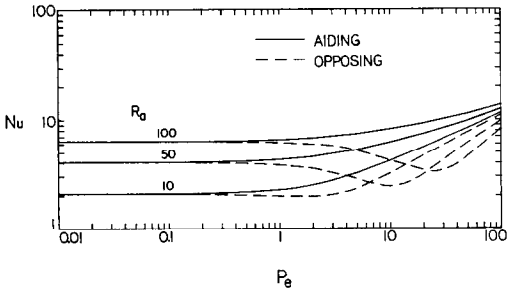

FIG. 13. Overall Nusselt number for aiding and opposing flows.

reattachment take place on the cold wall and the convective cell extends away from the heat source. However, in the case of opposing flow, the recirculation occurs on the heated wall. The strength and extent of the convective cell strongly depend on the governing parameters, and the higher the Rayleigh number, the larger the Peclet number required for the disappearance of the secondary flow.

It has been further shown that the local and overall heat transfer rates are complex functions of *Ra*, *Pe* and the direction of the main flow. A free convection regime has been characterized when the Nusselt number is a very weak function of the direction of main flow, and largely depends on Rayleigh number. The heat transfer rate in the mixed convection regime always increases with Peclet number provided the main flow aids buoyancy. The slope of the average Nusselt number curve depends on *Pe*, and increases from 0 to 0.5 as the flow regime changes from free to forced convection.

For opposing flow, the Nusselt number may, however, decrease with an increase in Peclet number from its free convection asymptote to a minimum before it starts increasing with *Pe*. This delays (in terms of *Pe*) the initiation of the forced convection regime. Also, it is possible that the Nusselt number for a lower Rayleigh number exceeds that for a higher *Ra* for certain combinations of the governing parameters.

Acknowledgements—The support of this work by the U.S. Nuclear Regulatory Commission under contract NRC-04-84-126 to the University of Delaware, and by the Columbia University is appreciated.

REFERENCES

1. R. A. Wooding, Convection in a saturated porous medium at large Rayleigh number and Peclet number, *J. Fluid Mech.* **15,** 527–544 (1963).
2. M. Prats, The effect of horizontal fluid flow on thermally induced convection currents in porous mediums, *J. Geophys. Res.* **71,** 4835–4837 (1966).
3. J. W. Elder, Steady free convection in a porous medium heated from below, *J. Fluid Mech.* **27,** 29–48 (1967).
4. M. A. Combarnous and P. Bia, Combined free and forced convection in porous media, *Soc. Petrol. Engrs J.* **11,** 399–405 (1971).
5. M. Jannot, P. Naudin and S. Vianny, Mixed convection in porous media, *Int. J. Heat Mass Transfer* **16,** 395–410 (1973).

6. P. J. Burns, L. C. Chow and C. L. Tien, Convection in a vertical slot filled with porous insulation, *Int. J. Heat Mass Transfer* **20,** 919–926 (1977).
7. P. Cheng, Combined free and forced convection flow about inclined surfaces in porous media, *Int. J. Heat Mass Transfer* **20,** 807–814 (1977).
8. P. Cheng, Similarity solutions for mixed convection from horizontal impermeable surfaces in saturated porous media, *Int. J. Heat Mass Transfer* **20,** 893–898 (1977).
9. C. T. Hsu and P. Cheng, The onset of longitudinal vortices in mixed convection flow over an inclined surface in a porous medium, *J. Heat Transfer* **102,** 544–549 (1980).
10. C. T. Hsu and P. Cheng, Vortex instability of mixed convective flow in a semi-infinite porous medium bounded by a horizontal surface, *Int. J. Heat Mass Transfer* **23,** 789–798 (1980).
11. W. J. Minkowycz, P. Cheng and R. N. Hirschberg, Nonsimilar boundary layer analysis of mixed convection about a horizontal heated surface in a fluid-saturated porous medium, *Int. Commun. Heat Mass Transfer* **11,** 127–141 (1984).
12. P. Ranganathan and R. Viskanta, Mixed convection boundary layer flow along a vertical surface in a porous medium, *Numer. Heat Transfer* **7,** 305–317 (1984).
13. R. N. Horne and M. J. O'Sullivan, Oscillatory convection in a porous medium: the effect of throughflow, 5th Austr. Conf. Hydr. Fluid Mech., New Zealand (1974).
14. P. Cheng and L. Tekchandani, The transient heating and withdrawal of fluids in a liquid-dominated geothermal reservoir, *The Earth's Crust*, Geophysical Monograph 20, pp. 705–721. Am. Geophys. Un. (1977).
15. P. Cheng and K. H. Lau, The effect of steady withdrawal of fluid in geothermal reservoirs, *Proc. 2nd UN Symp. Dev. and Use of Geoth. Resources*, Vol. 3, pp. 1591–1598 (1977).
16. V. E. Schrock and A. D. K. Laird, Physical modeling of combined forced and natural convection in wet geothermal formation, *J. Heat Transfer* **98,** 213–220 (1976).
17. J. Troncoso and D. R. Kassoy, An axisymmetric model for the charging of a liquid-dominated geothermal reservoir, *Int. J. Heat Mass Transfer* **26,** 1389–1401 (1983).
18. V. Prasad, F.-C. Lai and F. A. Kulacki, Mixed convection in horizontal porous layers heated from below, ASME Paper No. 86-HT-16 (1986); also, *J. Heat Transfer* (in press).
19. F.-C. Lai, V. Prasad and F. A. Kulacki, Effects of the size of heat source on mixed convection in horizontal porous layers heated from below, *Proc. 2nd ASME/JSME Thermal Engng Jt. Conf.*, Honolulu, Vol. 2, pp. 413–419 (1987).
20. F.-C. Lai, F. A. Kulacki and V. Prasad, Mixed convection in horizontal porous layers: effects of thermal boundary conditions. In *Mixed Convection Heat Transfer*—1987 (Edited by V. Prasad, I. Catton and P. Cheng), ASME HTD Vol. 84, pp. 91–96 (1987).
21. P. H. Oosthuizen, Mixed convection heat transfer from a horizontal plate in a porous medium near an impermeable surface. In *Natural Convection in Porous Media* (Edited by V. Prasad and N. A. Hussain), ASME HTD-Vol. 56, pp. 127–134 (1986).
22. M. Haajizadeh and C.-L. Tien, Combined natural and forced convection in a horizontal porous channel, *Int. J. Heat Mass Transfer* **27,** 799–813 (1984).
23. M. Parang and M. Keyhani, Boundary effects in laminar mixed convection flow through an annular porous medium. In *Natural Convection in Porous Media* (Edited by V. Prasad and N. A. Hussain), ASME HTD-Vol. 56, pp. 117–125 (1986).
24. A. D. Gosman, W. M. Pun, A. K. Runchal, D. B. Spalding and M. Wolfshtein, *Heat and Mass Transfer in Recirculating Flows*. Academic Press, New York (1969).
25. V. Prasad, Natural convection in porous media—an experimental and numerical study for vertical annular and rectangular enclosures, Ph.D. Dissertation, University of Delaware (1983).
26. V. Prasad, F. A. Kulacki and K. Stone, Free convection in a porous cavity with a finite wall heat source. In *Natural Convection in Enclosures*—1986 (Edited by R. S. Figliola and I. Catton), ASME HTD-Vol. 63, pp. 91–98 (1986).

CONVECTION MIXTE AIDEE OU GENEE DANS UNE COUCHE POREUSE VERTICALE AVEC UNE SOURCE DE CHALEUR A LA PAROI

Résumé—La convection mixte stationnaire bidimensionnelle dans une couche poreuse verticale est étudiée numériquement pour une source isotherme et finie de chaleur localisée sur une paroi verticale qui est ailleurs adiabatique et l'autre paroi étant isotherme et froide. Dans le cas de la convection mixte aidée, l'écoulement principal se détache de la paroi froide et il se forme une écoulement secondaire de recirculation dans une région écartée de la source de chaleur. Quand l'écoulement principal s'oppose au flottement, la séparation apparait sur la paroi chaude et l'écoulement secondaire est produit sur le segment chauffé. Bien que le flux thermique augmente avec la vitesse forcée favorable, l'effet est petit aux faibles nombres de Peclet (*Pe*). Pour l'écoulement forcé favorable, la pente de la courbe du nombre de Nusselt augmente avec le nombre de Peclet sauf lorsqu'on s'approche du régime de convection forcée pure. Pour l'écoulement opposé, le flux de chaleur décroît d'abord quand *Pe* augmente depuis zéro et il atteint un minimum avant qu'il augmente ensuite. Dans certaines conditions, le nombre de Nusselt pour un nombre de Rayleigh plus faible peut dépasser celui obtenu pour une valeur plus grande de *Ra*.

GLEICHGERICHTETE UND ENTGEGENGERICHTETE MISCHKONVEKTION IN EINER VERTIKALEN PORÖSEN SCHICHT MIT EINER ENDLICHEN WÄRMEQUELLE AN DER WAND

Zusammenfassung—Es wurde die zweidimensionale stationäre Mischkonvektion in einer vertikalen porösen Schicht numerisch für den Fall untersucht, daß eine endliche isotherme Wärmequelle an einer adiabaten senkrechten Wand angebracht ist, wobei die andere senkrechte Wand auf eine konstante Temperatur gekühlt wird. Bei gleichgerichteter Mischkonvektion löst die Hauptströmung von der kalten Wand ab, und es entsteht eine Sekundär-Rückströmung weit entfernt von der Wärmequelle. Bei gegengerichteter Mischkonvektion vollzieht sich die Ablösung an der beheizten Wand, und die Sekundärströmung bildet sich am beheizten Segment aus. Obwohl der Wärmeübergangskoeffizient durch die zusätzliche Geschwindigkeit größer wird, ist der Effekt bei kleineren Peclet-Zahlen (Pe) recht gering. Für die gleichgerichtete Strömung wird der Verlauf der Nusselt-Zahl mit wachsender Peclet-Zahl steiler, falls die Strömung sich noch nicht im Gebiet der erzwungenen Konvektion befindet. Bei der entgegengerichteten Strömung fällt der Wärmeübergang mit steigender Pe-Zahl zuerst unter Null ab und durchläuft ein Minimum, bevor er wieder ansteigt. Unter bestimmten Umständen kann die Nusselt-Zahl bei kleineren Rayleigh-Zahlen größer als bei höheren sein.

СО- И ПРОТИВОНАПРАВЛЕННАЯ СМЕШАННАЯ КОНВЕКЦИЯ В ВЕРТИКАЛЬНОМ ПОРИСТОМ СЛОЕ С КОНЕЧНОРАЗМЕРНЫМ ИСТОЧНИКОМ ТЕПЛА НА СТЕНКЕ

Аннотация—Численно исследовалась двумерная стационарная смешанная конвекция в вертикальном пористом слое в случае, когда конечноразмерный изотермический источник тепла находится на одной вертикальной стенке, которая является адиабатической в остальной своей части, а другая вертикальная стенка является изотермически холодной. В случае сонаправленной смешанной конвекции основной поток отрывается от холодной стенки, и на некотором расстоянии от источника тепла возникает вторичное рециркуляционное течение. Однако, когда основной поток направлен навстречу действия сил плавучести, отрыв происходит на нагретой стенке и вторичное течение возникает на нагреваемом участке. Несмотря на то, что интенсивность теплообмена увеличивается с ростом скорости сонаправленной конвекции, эффект оказывается незначительным при небольших значениях числа Пекле (Pe). При сонаправленном течении наклон кривой зависимости числа Нуссельта увеличивается с ростом числа Пекле при условии, что течение не вышло на режим вынужденной конвекции. В случае встречного течения интенсивность теплопереноса сначала уменьшается с ростом числа Pe от нулевого значения и выше, достигает минимума, а затем начинает расти. В некоторых случаях число Нуссельта при меньшем значении числа Рэлея может превышать значение, полученное при более высоком числе Ra.